THE JOURNAL OF BIOLOGICAL CHEMISTRY VOL. 289, NO. 15, pp. 10748–10760, April 11, 2014

Phosphoregulation of the Ceramide Transport Protein CERT at Serine 315 in the Interaction with VAMP-associated Protein (VAP) for Inter-organelle Trafficking of Ceramide in Mammalian Cells*

Received for publication, October 21, 2013, and in revised form, February 23, 2014 Published, JBC Papers in Press, February 25, 2014, DOI 10.1074/jbc.M113.528380

Keigo Kumagai, Miyuki Kawano-Kawada[1], and Kentaro Hanada[2]

From the Department of Biochemistry and Cell Biology, National Institute of Infectious Diseases, 1-23-1 Toyama, Shinjuku-ku, Tokyo 162-8640, Japan

Background: CERT transports ceramide from the ER to the Golgi apparatus and is supported by its FFAT motif-dependent binding to the ER membrane protein VAP.
Results: CERT is phosphorylated at Ser-315 near the FFAT motif.
Conclusion: The phosphorylation strengthens the CERT-VAP-A interaction to up-regulate ceramide trafficking.
Significance: This provides new insights into molecular mechanisms underlying functional regulation of FFAT-containing proteins for the inter-organelle lipid trafficking.

The ceramide transport protein CERT mediates the inter-organelle transport of ceramide for the synthesis of sphingomyelin, presumably through endoplasmic reticulum (ER)-Golgi membrane contact sites. CERT has a short peptide motif named FFAT, which associates with the ER-resident membrane protein VAP. We show that the phosphorylation of CERT at serine 315, which is adjacent to the FFAT motif, markedly enhanced the interaction of CERT with VAP. The phosphomimetic CERT S315E mutant exhibited higher activity to support the ER-to-Golgi transport of ceramide than the wild-type control in a semi-intact cell system, and this enhanced activity was abrogated when its FFAT motif was deleted. The level of phosphorylation of CERT at Ser-315 increased in HeLa cells treated with a sphingolipid biosynthesis inhibitor or exogenous sphingomyelinase. Expression of CERT S315E induced intracellular punctate structures, to which CERT and VAP were co-localized, and the occurrence of the structure was dependent on both phosphatidylinositol 4-monophosphate binding and VAP binding activities of CERT. Phosphorylation of another region (named a serine-rich motif) in CERT is known to down-regulate the activity of CERT. Analysis of various CERT mutant constructs showed that the de-phosphorylation of the serine-rich motif and the phosphorylation of Ser-315 likely have the additive contribution to enhance the activity of CERT. These results demonstrate that the phosphorylation of CERT at the FFAT motif-adjacent serine affected its affinity for VAP, which may regulate the inter-organelle trafficking of ceramide in response to the perturbation of cellular sphingomyelin and/or other sphingolipids.

Inter-organelle trafficking of lipids is fundamental to lipid metabolism and membrane biogenesis in eukaryotes. However, the molecular mechanisms of intracellular lipid trafficking and its regulation have not been elucidated in detail. Ceramide is the common precursor for various complex sphingolipids in mammalian cells (1–3). Ceramide is newly synthesized in the endoplasmic reticulum (ER)[3] and is transported to the *trans*-Golgi region for its conversion to sphingomyelin (SM) (3–5). Ceramide is also converted to glucosylceramide at the *cis*-Golgi region and/or a subregion of the ER (6). Glucosylceramide is converted to more complex glycosphingolipids in the *medial/trans*-Golgi regions (7, 8). The transport of ceramide from the ER to the Golgi site for the synthesis of SM is mediated by the ceramide transport protein CERT, a cytosolic 70-kDa protein (3, 9). CERT has several functional domains and motifs (Fig. 1*A*) as follows: (i) a pleckstrin homology (PH) domain capable of binding phosphatidylinositol 4-monophosphate (PtdIns(4)P) for Golgi targeting (9, 10); (ii) a steroidogenic acute regulatory protein-related (START) domain, which catalyzes the intermembrane transfer of ceramide (9, 11, 12); (iii) a short peptidic motif named "two phenylalanines in an acidic tract (FFAT)," capable of associating with VAMP-associated protein (VAP), an ER-resident membrane protein (13); and (iv) a serine-repeat motif (SRM), the phosphorylation of which represses the functions of both the PH and START domains (14). The role of CERT is supposed to rapidly transfer ceramide at the ER-to-Golgi membrane contact sites (9, 15). However, whether the interaction of CERT with VAP is regulated, and if so, how has

* This work was supported by Japan Society for the Promotion of Science KAKENHI Grants 23790118 and 25460086 (to K. K.), 22370054 and 25670045 (to K. H.), and by the Takeda Science Foundation.
[1] Present address: Integrated Center for Sciences, Dept. of Applied Bioresource Science, Faculty of Agriculture, Ehime University, Matsuyama 790-8566, Japan.
[2] To whom correspondence should be addressed. Tel.: 81-3-5285-1158; Fax: 81-3-5285-1157; E-mail: hanak@nih.go.jp.

[3] The abbreviations used are: ER, endoplasmic reticulum; CERT, ceramide transport protein; FFAT, two phenylalanines in an acidic tract; OSBP, oxysterol-binding protein; POPC, 1-palmitoyl-2-oleoyl-*sn*-glycerol-3-phosphocholine; POPE, 1-palmitoyl-2-oleoyl-*sn*-glycerol-3-phosphoethanolamine; PtdIns(4)P, phosphatidylinositol 4-monophosphate; SM, sphingomyelin; SRM, serine-repeat motif; START, steroidogenic acute regulatory protein-related lipid transfer; VAP, VAMP-associated protein; PH, pleckstrin homology; hCERT, human CERT; nHA, HA-tagged at the N terminus; TEV, tobacco etch virus.

not yet been elucidated. This study shows compelling evidence for the phosphorylation-dependent regulatory interaction of CERT with VAP in the ER-to-Golgi trafficking of ceramide and suggests this regulation is relevant to the ceramide transport via the ER-to-Golgi membrane contact sites.

EXPERIMENTAL PROCEDURES

Materials—Dulbecco's modified Eagle's medium (DMEM) and Ham's F-12 medium were purchased from Wako Pure Chemical Industries (Osaka, Japan). Lipofectamine®, PLUS™ reagent, Lipofectamine™ RNAiMAX, and NuPAGE® lithium dodecyl sulfate sample buffer (4×) were from Invitrogen. A mixture of protease inhibitors (Complete Protease Inhibitor Mixture Tablets) was from Roche Applied Science. Phosphatase inhibitor mixture 2 and phosphatase inhibitor mixture 3 were from Sigma. 1,2-Dioleoyl-*sn*-glycerol-3-phosphoethanolamine-*N*-lactosyl (ammonium salt), 1-palmitoyl-2-oleoyl-*sn*-glycerol-3-phosphocholine (POPC), 1-palmitoyl-2-oleoyl-*sn*-glycerol-3-phosphoethanolamine (POPE), and L-α-phosphatidylinositol-4-monophosphate were from Avanti Polar Lipids. Lactosylceramide was from Nagara Science (Gifu, Japan). *Ricinus communis* lectin (RCA 120) was from Vector Laboratories Inc. *N*-[*palmitoyl*-1-^{14}C]Palmitoyl-D-*erythro*-sphingosine ([^{14}C]ceramide) (55 mCi/mmol) was from American Radiolabeled Chemicals. ISP-1/myriocin (16) was a gift from Dr. Tetsuro Fujita (Research Institute for Production Development, Japan). Recombinant *Bacillus cereus* sphingomyelinase was from Higeta Shoyu (Tokyo, Japan). Small interfering RNA was from Hokkaido System Science (Sapporo, Japan). The following antibodies were purchased: rat monoclonal anti-HA and rat monoclonal anti-HA horseradish peroxidase (HRP)-conjugated (Roche Applied Science); rabbit polyclonal anti-protein-disulfide isomerase, mouse monoclonal anti-FLAG HRP-conjugated, anti-FLAG antibody-coupled agarose, and anti-HA antibody-coupled agarose (Sigma); mouse monoclonal anti-GS28 (StressGen); mouse monoclonal anti-GM130 and anti-EEA1 (BD Biosciences); rabbit polyclonal anti-Sec61β (Merck); rabbit monoclonal anti-LAMP1 and anti-syntaxin-6 (Cell Signaling); and secondary antibodies conjugated to Alexa Fluor 488 and Alexa Fluor 594 (Invitrogen).

Antibodies—A polyclonal antibody against Ser(P)-315 of human CERT was generated by the immunization of rabbits with the synthetic phosphopeptide CEEGPN(pS)LINEE (residues 310–320 plus a cysteine) conjugated to keyhole limpet hemocyanin using the manufacturer's standard protocol (Scrum Inc., Tokyo, Japan). A part of the antiserum was affinity-purified by binding to CNBr-activated Sepharose™ 4B (GE healthcare) conjugated with the phosphopeptide (CEEGPN(pS)LINEE) and passing through that with a nonphosphopeptide (CEEGPNSLINEE). A chicken polyclonal antibody against human VAP-A was generated by the immunization of chickens with the purified recombinant protein of VAP-A (3–269) using the manufacturers' standard protocol (Scrum Inc., Tokyo, Japan). A part of the antiserum was affinity-purified by binding to CNBr-activated Sepharose™ 4B (GE Healthcare) conjugated with purified VAP-A (3-269).

Construction of HA-tagged CERT Mutants—Ser-315-related CERT mutants tagged with the HA epitope were constructed by PCR with the pBluescript® II SK(+) (Agilent Technologies)-based plasmid pBS/nHA-hCERT WT (14) (nHA indicates HA-tagged at the N terminus, and hCERT indicates human CERT), as a template and sets of primers as follows: nHA-hCERT S315A, 5′-GAAGGCCCTAACGCTCTGATTAATGAAGAA-3′ and 5′-TTCATTAATCAGAGCGTTAGGGCCTTCTTC-3′; nHA-hCERT S315D, 5′-GAAGGCCCTAACGATCTGATTAATGAAGAA-3′ and 5′-TTCATTAATCAGATCGTTAGGGCCTTCTTC-3′; nHA-hCERT S315E, 5′-GAAGGCCCTAACGAACTGATTAATGAAGAA-3′ and 5′-TTCATTAATCAGTTCGTTAGGGCCTTCTTC-3′. cDNA fragments containing the mutated site were subcloned into the MluI/XhoI site of pBS/nHA-hCERT WT to make pBS/nHA-hCERT S315A, pBS/nHA-hCERT S315D, and pBS/nHA-hCERT S315E, respectively. cDNA fragments encoding mutated nHA-hCERT were then subcloned from the pBluescript vector into the EcoRI/XhoI sites of pcDNA3.1(+)Neo (Invitrogen) to make pcDNAneo/nHA-hCERT S315A, pcDNAneo/nHA-hCERT S315D, and pcDNAneo/nHA-hCERT S315E, respectively. cDNA fragments encoding the mutated nHA-hCERT were also subcloned into the EcoRI/XhoI site of pET28a(+) (Merck). A previously described pcDNA3.1/nHA-hCERT G67E vector (14) was digested with MluI, and the fragment (1.4 kb) containing the G67E mutation was nondirectionally subcloned into the MluI/MluI sites of pcDNAneo/nHA-hCERT S315E. Desired orientation of the insert was confirmed by the appearance of a 1.8-kb fragment after digestion of obtained plasmids with EcoRI and XhoI, and the resultant plasmid was used as pcDNAneo/nHA-hCERT G67E/S315E. Previously described pBS/hCERT$_L$ (9) and pBS/nFL-hCERT D324A (13) vectors were digested with MluI/XhoI and subcloned into the corresponding region of pBS/nHA-hCERT WT to make pBS/nHA-hCERT$_L$ and pBS/nHA-hCERT D324A, respectively. cDNA fragments encoding nHA-hCERT$_L$ and nHA-hCERT D324A were then subcloned into the EcoRI/XhoI sites of pcDNA3.1(+)Neo to make pcDNAneo/nHA-hCERT$_L$ and pcDNAneo/nHA-hCERT D324A, respectively. pcDNAneo/nHA-hCERT G67E/S132A was described previously (14). pcDNAneo/nHA-hCERT S132A and pcDNAneo/nHA-hCERT 10E vectors, which have been used in a previous study (14), were digested with MluI, and the fragment (1.4 kb) containing the S132A or 10E mutation was nondirectionally subcloned into the MluI/MluI sites of pcDNAneo/nHA-hCERT S315A or pcDNAneo/nHA-hCERT S315E to make pcDNAneo/nHA-hCERT S132A/S315A, pcDNAneo/nHA-hCERT 10E/315A, pcDNAneo/nHA-hCERT S132A/S315E, and pcDNAneo/nHA-hCERT 10E/S315E, respectively. The desired orientation of the insert was confirmed by sequencing the plasmid.

Construction of HA-CERT ΔFFAT Mutants—A cDNA fragment encoding FFAT-deleted hCERT was subcloned from pBS/nFL-hCERT ΔFFAT (13) into the HindIII/XhoI site of pBS/nHA-hCERT WT to attach the HA tag at the N terminus (the resultant plasmid was pBS/nHA-hCERT ΔFFAT). cDNA fragments encoding nHA-hCERT ΔFFAT were then subcloned from pBS/nHA-hCERT ΔFFAT into the EcoRI/XhoI site of pcDNA3.1(+)Neo and pET28a(+) to make pcDNAneo/nHA-hCERT ΔFFAT and pET/nHA-hCERT ΔFFAT, respectively. A cDNA fragment of nHA-hCERT S315E/ΔFFAT was constructed by PCR with pcDNAneo/nHA-hCERT S315E as a template and a set

of primers (5′-AATGAAGAAGCTGCTCTTGACAGAC-3′ and 5′-AGCAGCTTCTTCATTAATCAGTTCGT-3′). The cDNA fragment encoding nHA-hCERT S315E/ΔFFAT was subcloned into the EcoRI/XhoI sites of pcDNA3.1(+)Neo to make pcDNAneo/nHA-hCERT S315E/ΔFFAT. The cDNA fragment (nHA-hCERT S315E/ΔFFAT) was also subcloned into the EcoRI/XhoI sites of pET28a(+) to make pET/nHA-hCERT S315E/ΔFFAT.

Construction of FLAG-tagged VAP-A for Expressing in Mammalian Cells—The cDNA fragment encoding human VAP-A was amplified by PCR with pBS/kzHA-VAP-A (13) as a template and a set of primers (5′-CCCAAGCTTCCATGGCGAAGCACG-3′ and 5′-TAAGTCGACCTACAAGATGAATTTCCCTAGAAAG-3′). PCR products were digested with HindIII/SalI and subcloned into the HindIII/XhoI sites of the pBS-nFLcHA vector (13) to attach the FLAG tag at the N terminus. cDNA encoding FLAG-tagged human VAP-A was then subcloned into the NotI/ApaI sites of pcDNA3.1(+)Hygro (Invitrogen) to make pcDNAhyg/nFL-hVAP-A.

Construction of a Plasmid for Bacterial Expression of a Transmembrane Domain-less VAP-A—The full size (294 amino acid residues) of the open reading frame (ORF) sequence of human VAP-A was obtained by PCR with a cDNA library of HeLa cells (Invitrogen) as the template and a set of primers (5′-CAGAATTCATGGCGTCCGCCTCAGG-3′ and 5′-TAAGTCGACCTACAAGATGAATTTCCCTAGAAAGAATCC-3′). After digestion with EcoRI/SalI, the amplified fragment was cloned into the EcoRI/SalI sites of the pBluescript vector to produce the plasmid pBS/hVAP-A. The ORF for a TEV protease-cleavable VAP-A derivative without the transmembrane region was then constructed by PCR with pBS/hVAP-A as the template and set of primers (5′-CAGAATTCGAAAACCTGTACTTTCAGTCCGCCTCAGGGGCC-3′ and 5′-TAAGTCGACCTAGACATTATCTCTGAAGGATGCAG-3′). After digestion with EcoRI/SalI, the amplified fragment was cloned into EcoRI/SalI sites of the pET-28a(+) vector to produce pET/TEV-hVAP-A ΔTM. Its ORF encoded the 3–259-amino acid region of human VAP-A.

Cell Culture and Transfection—HeLa-S3 cells were maintained in DMEM supplemented with 10% fetal bovine serum, 100 units/ml penicillin G, and 100 μg/ml streptomycin sulfate at 37 °C in a humidified atmosphere containing 5% CO_2. CHO-K1 cells were cultured in Ham's F-12 medium supplemented with 10% newborn calf serum, 100 units/ml penicillin G, and 100 μg/ml streptomycin sulfate at 37 °C. Cells were transfected with plasmids with Lipofectamine® and PLUS™ reagent according to the manufacturer's instructions. To obtain stable transformants, pcDNAneo/nHA-hCERT WT constructs were digested with PvuI, and the linearized plasmid was transfected into HeLa-S3 cells. Cells were then cultured in medium containing 0.5 mg/ml G418. Cells were transfected with siRNA with Lipofectamine® RNAiMAX reagent according to the manufacturer's instructions.

Co-immunoprecipitation of HA-tagged CERT and FLAG-tagged VAP-A—Co-immunoprecipitation was performed with a modified method as described previously (13). Briefly, cells cultured in 100-mm diameter dishes were transiently co-transfected with pcDNAneo/nHA-hCERT and pcDNAhyg/nFL-hVAP-A by using Lipofectamine® and Plus™ reagent. After incubation for 24 h, the subconfluent cells were rinsed with phosphate-buffered saline (PBS) and harvested in buffer A (50 mM Tris-HCl (pH 7.4), 1 mM EDTA, 1 mM EGTA, 100 mM NaCl, 50 mM NaF, 5 mM sodium pyrophosphate, 10 mM disodium-β-glycerophosphate, a mixture of protease inhibitors (1 tablet/50 ml), 1% phosphatase inhibitor mixture 2, and 1% phosphatase inhibitor mixture 3). CHO-K1 cells were incubated on ice for 45 min in 120 μl of 0.5% digitonin/buffer A, or HeLa-S3 cells were incubated for 20 min in 420 μl of 1.0% Triton X-100/buffer A. The extracts were clarified by centrifugation at 20,000 × *g* for 10 min at 4 °C. Equal amounts of proteins were incubated with anti-FLAG antibody-coupled agarose or anti-HA antibody-coupled agarose for 1 h at 4 °C with gentle shaking. The resin was precipitated by centrifugation at 1000 × *g*, rinsed three times with buffer C (50 mM Tris-HCl (pH 7.4), 1 mM EDTA, 1 mM EGTA, 100 mM NaCl, 50 mM NaF, 5 mM sodium pyrophosphate, 10 mM disodium-β-glycerophosphate, a mixture of protease inhibitors (1 tablet/50 ml), with 0.01% digitonin) (for CHO-K1 cells) or buffer A with 0.1% Triton X-100 (for HeLa-S3 cells). The resin was incubated in 50 μl of 1× NuPAGE® lithium dodecyl sulfate sample buffer with 50 mM dithiothreitol at 70 °C for 10 min. After centrifugation at 1000 × *g*, the supernatant was subjected to Western blotting as the immunoprecipitated fraction.

Western Blotting—Proteins dissolved in NuPAGE® lithium dodecyl sulfate sample buffer (1×) with 50 mM dithiothreitol were separated by SDS-PAGE and transferred to polyvinylidene difluoride membrane (Bio-Rad). The membrane was incubated with various primary antibodies diluted in 1% nonfat milk in 0.1% Tween 20/Tris-buffered saline (TBS). To detect the phosphorylation of Ser-315, the membrane was incubated with the purified anti-Ser(P)-315 antibody diluted in 3% bovine serum albumin (BSA) in 0.1% Tween 20/TBS in the presence of 100 nM nonphosphopeptide (CEEGPNSLINEE). When using a crude antiserum against Ser(P)-315, a higher concentration (5 μM) of the nonphosphopeptide was added. After incubation with secondary antibodies in 3% BSA in 0.1% Tween 20/TBS, the membrane was subjected to Immobilon Western chemiluminescent HRP substrate (Millipore) and exposed to x-ray films or imaged by LAS-1000 plus (GE Healthcare).

Assay of the ER-to-Golgi Transport of Ceramide in Semi-intact Cells—The assay was performed as described previously (9, 17, 18). Briefly, perforated LY-A cells, in which [^{3}H]ceramide was pre-formed in the ER by metabolic labeling with [^{3}H]sphingosine at 15 °C, were chased in the presence of the cytosol fraction of LY-A cells, an ATP-regenerating system, and purified CERT at 37 °C, and [^{3}H]SM formed was determined as the measure of the activity.

Cell-free Assay of the Intermembrane Transfer of Ceramide—A cell-free assay of the intermembrane transfer of ceramide was performed with modifications according to a previously reported method (9, 11). Briefly, donor and acceptor liposomes composed of POPC/POPE/dioleoyl-*sn*-glycerol-3-phosphoethanolamine-*N*-lactosyl (ammonium salt)/[^{14}C]ceramide (55 mCi/mmol) (64:16:40:1, mol/mol) and POPC/POPE (4:1, mol/mol), respectively, were formed in buffer C (20 mM Hepes-NaOH (pH 7.4) containing 50 mM NaCl and 1 mM EDTA) by probe-type sonication. The acceptor liposomes were pre-centrifuged at 20,000 × *g* for 5 min at 4 °C, and the supernatant fraction was used for the assay. Donor liposomes (60.5 nmol/20

μl/assay), acceptor liposomes (400 nmol/60 μl/assay), and purified recombinant CERT (2 pmol) were incubated in 100 μl of buffer C at 37 °C for 10 min. After the addition of 30 μl of 1.25 mg/ml of RCA 120 to the reaction mixture, the resultant mixture was incubated on ice for 15 min to aggregate donor liposomes, and it was then centrifuged at 20,000 × *g* for 3 min at 4 °C. The radioactivity of the supernatant was determined as a measure of the ceramide transferred to acceptor liposomes.

PtdIns(4)P Binding Assay—PtdIns(4)P binding activity was assayed by a modification of the previously reported method (14). Purified CERT was pre-centrifuged at 20,000 × *g* for 10 min at 4 °C on the day of the assay, and the supernatant was used for the assay. Liposomes composed of POPC/POPE/lactosylceramide (16:4:6, mol/mol) with various amounts of PtdIns(4)P were formed in buffer C by probe-type sonication. Purified CERT (200 fmol) was incubated with the liposomes (26 nmol/20 μl/assay) in 50 μl of binding buffer (buffer C containing 0.3 mg/ml BSA and 0.1% CHAPS) at 4 °C for 30 min. After the addition of 15 μl of 1.25 mg/ml RCA 120, the mixture was incubated on ice for 10 min to aggregate liposomes. Liposomes were then precipitated by centrifugation at 20,000 × *g* for 3 min at 4 °C. The amount of CERT in the supernatant and pellet fractions was determined by Western blotting with the HRP-conjugated anti-HA antibody, and the ratio of the precipitated to the total (pellet/(pellet + supernatant)) was calculated.

Immunofluorescence Microscopy—Manipulations were done at room temperature unless otherwise noted. HeLa-S3 cells were grown on coverslips at 37 °C, fixed in Mildform® 10N (4% formaldehyde in PBS) (Wako Pure Chemical Industries) for 15 min, and incubated with 0.1 M NH_4Cl in PBS for 10 min. The fixed cells were permeabilized with 0.1% Triton X-100/PBS for 10 min and blocked with 3% BSA/PBS for 16 h at 4 °C. Cells were then incubated with primary antibodies diluted in 0.1% BSA/PBS (1:250) for 2 h, washed with PBS, and incubated with secondary antibodies diluted in 0.1% BSA/PBS (1:400) for 2 h. After two washes with PBS, the coverslips were mounted on Fluoromount™ (Diagnostic BioSystems), and images were captured using a confocal laser-scanning microscope (Axiovert 200 M; Carl Zeiss) equipped with an LSM 510 system (Carl Zeiss) using both 488- and 543-nm excitations and a C-Apochromat 63×/1.2-watt Corr water-immersion objective lens. Images were prepared using LSM software (Carl Zeiss) and further processed using Photoshop software.

Purification of Recombinant Proteins—Bacterial expression plasmids pET-28a(+) encoding His_6-tagged CERT WT, CERT mutants, or TEV-VAP-A ΔTM were transfected into *Escherichia coli* BL21 (DE3) cells. We prepared lysates from the transfected cells as described (19). His_6-tagged proteins were purified from the lysate using a Talon Co^{2+} affinity column (Clontech) as described (9, 17). The purified His_6-tagged CERT WT and CERT mutants were used for the assay, and TEV-VAP-A ΔTM was further processed for an immunization antigen. The purified TEV-VAP-A ΔTM protein was incubated with polyhistidine-tagged AcTEV™ protease (Invitrogen) at 30 °C for 16 h to remove the His_6 tag from VAP-A ΔTM. After removal of AcTEV™ protease by incubating with TALON resin, the solution unbound to the resin was collected, and its solvent was substituted for PBS by centrifugal filter units (Millipore). The resultant fraction was used as purified VAP-A ΔTM for immunization of chickens. In our preliminary trials to prepare anti-VAP-A antibody with a His_6 tag VAP-A ΔTM protein as an antigen, the antisera obtained likely reacted with ~25 amino acid residues encoded by DNA sequence between the N-terminal His_6 tag region and the multicloning site in the pET vector. This problem was solved by using the TEV-employed procedure described above.

Immunopurification of HA-tagged CERT—HA-tagged CERT versions were purified from transiently overexpressing cells by affinity chromatography. HeLa-S3 cells (60–80% confluent) in a 150-mm dish were transfected with plasmids encoding HA-tagged CERT WT or mutant CERT using Lipofectamine PLUS reagents and cultured for 24 h. All subsequent manipulations were performed at 4 °C or on ice unless otherwise indicated. Cells were washed twice with 4 ml of phosphate-buffered saline and once with 2 ml of buffer B (50 mM Tris-HCl (pH 7.4) containing 100 mM NaCl, 1 mM Na_2EDTA, 5 mM sodium pyrophosphate, 50 mM NaF, 1 mM sodium orthovanadate, and 1 tablet of protease inhibitor mixture (Roche Applied Science)/50 ml). The cells were then scraped in buffer B (~1000 μl), and 20% (w/v) Triton X-100 was added to a final concentration of 1% (w/v). Cells were incubated for 20 min, and the lysates were centrifuged at 20,000 × *g* for 10 min. The supernatant fractions were incubated with 30 μl of a 50% slurry of anti-HA antibody-conjugated agarose for 2 h with gentle shaking. Agarose was washed twice with 1 ml of buffer B supplemented with 0.1% Triton X-100 and three times with buffer C (20 mM Tris-HCl (pH 7.4) containing 500 mM NaCl). It was then suspended in 60 μl of buffer C supplemented with 1 μg/μl HA peptides (Sigma) and incubated overnight for elution. After a brief centrifugation, the supernatant was collected, and 2 M sucrose was added to a final concentration of 250 mM. The purified CERT fraction was divided into aliquots and stored at −80 °C.

RESULTS

Phosphorylation of Serine 315 Adjacent to the FFAT Motif of CERT—Our previous study suggested that only a small portion of input wild-type CERT protein could form a tight complex with VAP in co-immunoprecipitation experiments (13), which raised the possibility that the CERT-VAP interaction may be controlled in cells. The canonical FFAT motif has been suggested to divide into two regions, a core region composed of 7 amino acids EFFDA*X*E and an acidic flanking region around the core region, and that also the CERT-VAP interaction may start with an initial electrostatic interaction between the acidic flanking region and basic electropositive face of VAP followed by binding of the core region with VAP in a "lock-and-key" manner (20, 21). A phosphoproteome study by Olsen *et al.* (22) revealed the phosphorylation of CERT at serine 315 (Ser-315) in an acidic flanking region of the FFAT motif (Fig. 1*A*). Thus, we decided to elucidate whether the phosphorylation of CERT at Ser-315 affected the CERT-VAP interaction. We prepared an antibody against a synthetic peptide (CEEGPN(pS)LINEE) corresponding to amino acids 310–320 of CERT with phosphorylated Ser-315 (Ser(P)-315) (Fig. 1*A*). Human cervical HeLa-S3 cells (ATCC CCL2.2) were transfected with plasmids encoding HA-tagged wild-type CERT (HA-CERT WT) or the HA-CERT

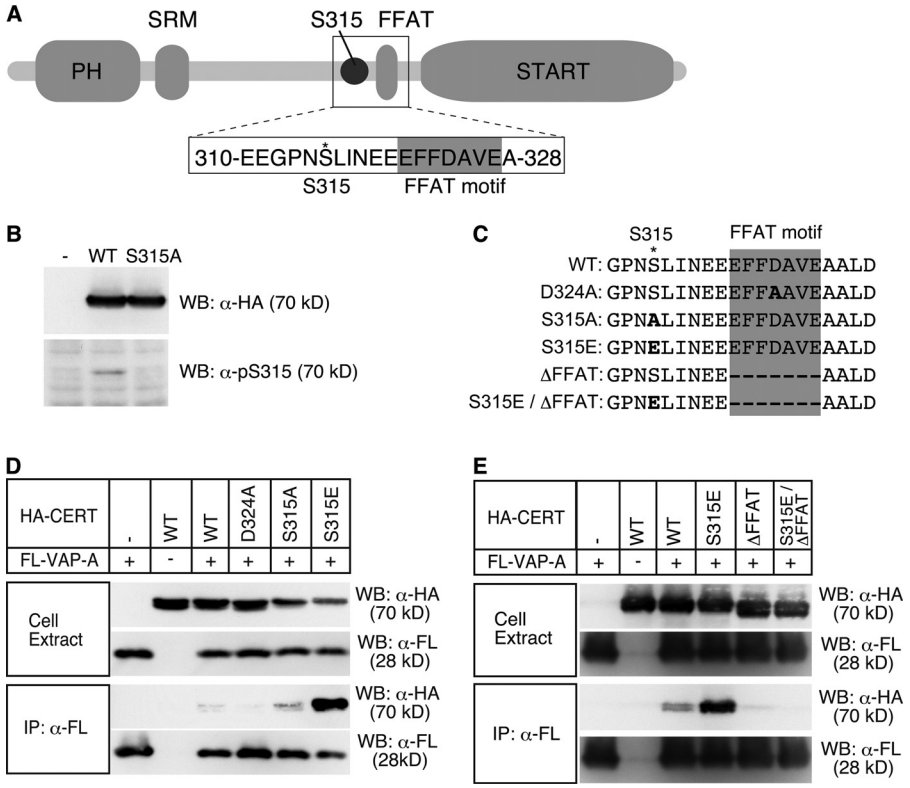

FIGURE 1. **Enhancement of the CERT-VAP interaction by phosphomimetic mutation at Ser-315 of CERT.** *A,* schematic view of the structure of human CERT and the amino acid sequence containing Ser-315 near the FFAT motif (GenBank™ accession number NP_112729). The core region of the FFAT motif is highlighted by a *gray box*, and the *asterisk* represents the position of Ser-315. *B,* HeLa-S3 cells were transfected with an expression plasmid encoding HA-CERT WT, HA-CERT S315A, or an empty vector and cultured for 48 h before harvesting. Cell lysates were prepared with previously described lysis buffer (29) and subjected to SDS-PAGE followed by Western blotting (*WB*) with the anti-HA antibody (*α-HA*) and anti-Ser(P)-315 antibody (*α-pS315*). The experiments were performed at least three times, and similar results were obtained. Typical blot patterns are shown. *C,* amino acid sequences (312–331) around the FFAT motif of various human CERT constructs are shown. The core region of the FFAT motif is highlighted by a *gray box*; an *asterisk* represents the position of Ser-315, and the mutated residues are in *bold letters*. *D,* digitonin extracts were prepared from CHO-K1 cells co-expressing the indicated HA-CERT constructs and FLAG-VAP-A (*FL-VAP-A*). FLAG-VAP-A was immunoprecipitated (*IP*) from extracts with the anti-FLAG antibody (*α-FL*) and analyzed by Western blotting with the indicated antibodies. Experiments were performed at least three times, and similar results were obtained. *E,* Triton X-100 extracts were prepared from HeLa-S3 cells co-expressing the indicated HA-CERT constructs and FLAG-VAP-A. FLAG-VAP-A was immunoprecipitated from the extracts and analyzed by Western blotting with the indicated antibodies.

S315A mutant, and cells were then lysed with the nonionic detergent Triton X-100 for Western blotting analysis with an anti-hemagglutinin (HA) or anti-Ser(P)-315 antibody. Although the expression levels of HA-CERT WT and HA-CERT S315A were nearly equivalent, the anti-Ser(P)-315 antibody detected HA-CERT WT, but not HA-CERT S315A, which indicated that CERT expressed in HeLa-S3 cells was phosphorylated at Ser-315 (Fig. 1*B*). The phosphorylation of CERT at Ser-315 was also detected in other cells types, including HeLa (ATCC CCL2), HEK293, and CHO-K1 cells (data not shown).

CERT Ser-315 Phosphorylation Enhanced the FFAT-dependent Association of CERT with VAP—To examine whether the phosphorylation of CERT at Ser-315 could affect the CERT-VAP interaction, CHO-K1 cells were transfected with plasmids encoding the various HA-CERT constructs (Fig. 1*C*) and FLAG-tagged wild-type human VAP-A (FL-VAP-A) and lysed with the mild detergent digitonin. The expression levels of FL-VAP-A were nearly equivalent among the transfected cells, and those of the HA-CERT constructs were also comparable among them (Fig. 1*D*). FL-VAP-A was immunoprecipitated with the anti-FLAG antibody from the lysates, and immunoprecipitated fractions were analyzed by Western blotting with various antibodies. HA-CERT WT was marginally co-precipitated with FL-VAP-A and HA-CERT D324A, which was deficient in VAP binding activity, and was not co-precipitated as indicated previously (Fig. 1*D*) (13). Under such conditions, HA-CERT S315E, a mutant that is expected to mimic the Ser-315-phosphorylated state, was very effectively coprecipitated with FL-VAP-A, whereas HA-CERT S315A, a nonphosphorylatable mutant, was coprecipitated to a similar level as HA-CERT WT (Fig. 1*D*). The apparent molecular mass of FL-VAP-A on Western blots was estimated to be ~28 kDa despite its deduced molecular mass of 33 kDa. This discrepancy was attributed to the irregular mobility of hydrophobic proteins in SDS-PAGE (23).

We tested whether the increased association of HA-CERT S315E with VAP-A required the core region (EFFDAVE) of the FFAT motif. After the transfection of HeLa-S3 cells with plasmids encoding the HA-CERT constructs and FL-VAP-A, cells were lysed with Triton X-100. Similar expression levels were observed among the constructs used (Fig. 1, *C* and *E*). FL-VAP-A was immunoprecipitated with the anti-FLAG antibody from the lysates, and immunoprecipitated fractions were analyzed by Western blotting with various antibodies. When compared with the wild-type CERT control, a markedly higher

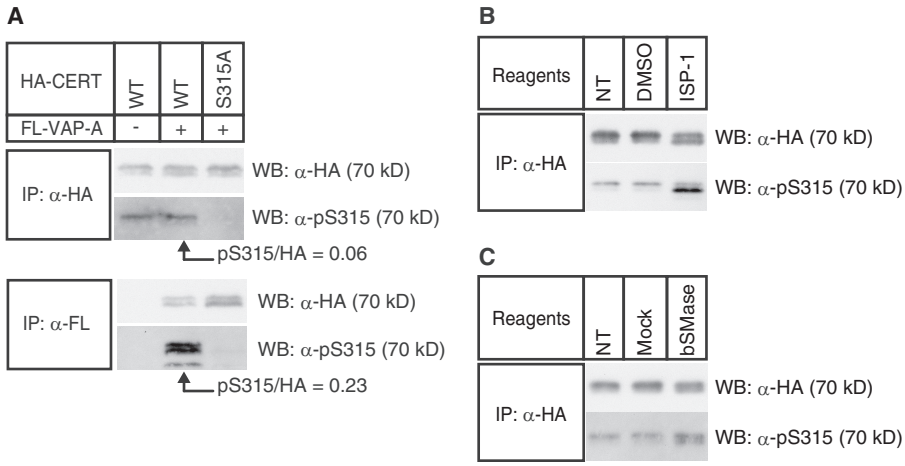

FIGURE 2. **Phosphorylation state of wild-type CERT at Ser-315.** *A,* Triton X-100 extracts were prepared from HeLa-S3 cells co-expressing the indicated HA-CERT constructs and FLAG-VAP-A (*FL-VAP-A*). HA-CERT or FLAG-VAP-A was immunoprecipitated (*IP*) from the extracts with the indicated antibody. The abundance of HA-CERT proteins in the immunoprecipitated fractions was quantified by Western blotting (*WB*) with the anti-HA antibody, and these fractions were then diluted with sample buffer to adjust the loading amounts of HA-CERT for comparisons between immunoprecipitated fractions with anti-HA and anti-FLAG antibodies. Loaded volumes of anti-HA and anti-FLAG immunoprecipitated fractions were equivalent to 0.04 and 4 μl of the original fraction, respectively. CERT was detected by Western blotting with anti-HA antibody or anti-Ser(P)-315 antiserum. Experiments were performed at least twice, and similar results were obtained. *B,* HeLa-S3 cells stably expressing HA-CERT WT were treated with 5 μM ISP-1, mock-treated (dimethyl sulfoxide, DMSO), or nontreated (*NT*) for 24 h in serum-free DMEM. Triton X-100 extracts were prepared from the cells, and HA-CERT WT was immunoprecipitated from extracts with the anti-HA antibody, and precipitated CERT was detected by Western blotting with the anti-HA antibody and anti-Ser(P)-315 antiserum. Experiments were performed at least twice, and similar results were obtained. *C,* HeLa-S3 cells stably expressing HA-CERT WT were treated with 30 milliunits/ml *B. cereus* sphingomyelinase (*bSMase*), mock-treated (40% glycerol), or nontreated (*NT*) for 2 h in serum-free DMEM. HA-CERT WT was immunoprecipitated and analyzed by Western blotting as described in *B*. Experiments were performed twice, and similar results were obtained.

amount of HA-CERT S315E was co-immunoprecipitated with FL-VAP-A, whereas the deletion of its FFAT motif (CERT S315E/ΔFFAT) was not co-immunoprecipitated (Fig. 1*E*), which indicated that the core region of the FFAT motif was indispensable for enhancing the CERT-VAP interaction by the phosphorylation of CERT at Ser-315.

Ser-315-phosphorylated Form of Wild-type CERT Exhibited a High Affinity for VAP in Cells—We next attempted to determine whether the phosphorylation of wild-type CERT at Ser-315 affected its affinity for VAP in cells. If the CERT-VAP interaction was strengthened by the phosphorylation of CERT at Ser-315, CERT with phosphorylated Ser-315 should be more enriched in a fraction coprecipitated with VAP-A than a fraction containing the whole CERT. To test this hypothesis, HA-CERT WT or HA-CERT S315A was co-expressed with FL-VAP-A in HeLa-S3 cells and immunoprecipitated with the anti-HA or anti-FLAG antibody. The ratios of Ser-315-phosphorylated CERT to whole CERT in the immunoprecipitated fractions were then analyzed by Western blotting (Fig. 2*A*). In the HA-immunoprecipitated fractions, the anti-Ser(P)-315 antibody reacted with 70-kDa bands when HA-CERT WT, but not HA-CERT S315A mutant, was expressed (Fig. 2*A*), which confirmed the specific recognition of Ser-315-phosphorylated HA-CERT WT. In the FLAG-immunoprecipitated fractions, the anti-Ser(P)-315 antibody more densely reacted with 70-kDa bands corresponding to Ser-315-phosphorylated HA-CERT WT (Fig. 2*A*). The ratio of the chemiluminescence intensity (Ser(P)-315/HA), which represents the enrichment of Ser-315-phosphorylated CERT in the complex with VAP-A, was estimated to be 3.8-fold higher in the FLAG-coprecipitated fraction than in the HA-immunoprecipitated fraction. Therefore, we concluded that the Ser-315 phosphorylation of CERT strengthened the CERT-VAP interaction, which was consistent with the results obtained using the CERT S315E construct.

Phosphorylation State of CERT at Ser-315 Was Affected by the Perturbation of SM in Cells—We next investigated whether the phosphorylation state of CERT at Ser-315 changed in response to the demand for SM. HeLa-S3 cells stably expressing HA-CERT WT were treated with 5 μM ISP-1 (myriocin), a potent inhibitor of sphingolipid biosynthesis, or were mock-treated (dimethyl sulfoxide). HA-CERT WT immunoprecipitated with the anti-HA antibody was analyzed by Western blotting with the anti-HA antibody (to examine total HA-CERT levels) and anti-Ser(P)-315 CERT antibodies (to examine the levels of the Ser-315-phosphorylated form) (Fig. 2*B*). The treatment of cells with ISP-1 altered the doublet pattern of CERT WT, namely an increment in a lower band and coincident decrement in an upper band (Fig. 2*B*), which was consistent with our previous study (14) (see under "Discussion"). The ISP-1 treatment enhanced the phosphorylation state of Ser-315, especially in the lower band, whereas the mock treatment did not affect the phosphorylation state at Ser-315 (Fig. 2*B*). An increase in the phosphorylation of Ser-315 was also observed when cells were treated with exogenous sphingomyelinase for 2 h (Fig. 2*B*), although the increment induced by sphingomyelinase was markedly less than that induced by ISP-1 (Fig. 2, *B* and *C*). These results suggested that the phosphorylation state of CERT at Ser-315 was affected in response to the perturbation of cellular sphingomyelin and/or other sphingolipids.

Phosphorylation at Ser-315 Up-regulated CERT-mediated Transport of Ceramide from the ER to the Golgi Apparatus—We next addressed the effect of phosphorylation at Ser-315 on the CERT-mediated transport of ceramide from the ER to the Golgi apparatus for the synthesis of SM. An *in vitro* reconstitu-

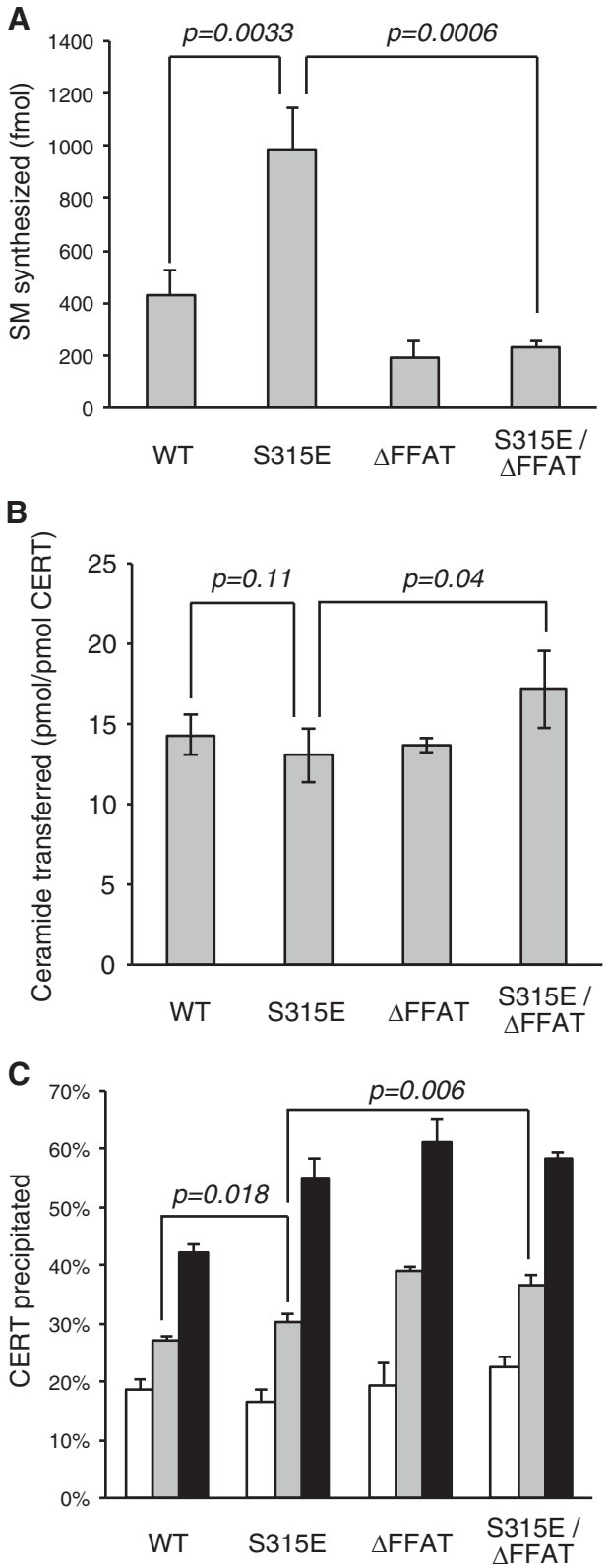

FIGURE 3. **Effects of the phosphomimetic mutation of CERT at Ser-315 on CERT functions.** *A,* CERT WT and CERT mutants expressed in *E. coli* BL21 (DE3) cells were purified. The purified CERT proteins (20 fmol) were used to measure the activity of mediating the ER-to-Golgi trafficking of ceramide in semi-intact LY-A cells as described previously (18). The data shown are the means ± S.D. from three experiments. Significance of changes was analyzed by Student's *t* test, and *p* values are shown. *B,* inter-membrane ceramide transfer activity of purified CERT proteins was measured in a cell-free system using artificial phospholipid vesicles. The data shown are the means ± S.D. from three experiments. Significance of changes was analyzed by Student's *t* test, and *p* values are shown. *C,* purified CERT proteins were examined on their binding to liposomes containing various amounts of PtdIns(4)P. The percentage of the amount of co-precipitated CERT relative to the total was estimated. Without PtdIns(4)P is shown by *white bars*; 0.1% PtdIns(4)P is shown by *light gray bars*; and 0.3% PtdIns(4)P is shown by *dark gray bars*. The data shown are the means ± S.D. from three experiments. Significance of changes was analyzed by Student's *t* test, and *p* values are shown.

tion assay system within semi-intact CHO cells was shown to reproduce various aspects of the ER-to-Golgi trafficking of ceramide (9, 13, 17, 18). This reconstitution method allowed us to adjust the quantity of CERT proteins added to the assay system. Various types of CERT proteins purified from a bacterial expression system were examined for activity to support ceramide trafficking in semi-intact CHO mutant cells (LY-A cells), in which endogenous CERT was genetically impaired (9). The CERT recombinants used here were purified from *E. coli* cells. Note that phosphorylation of human proteins in *E. coli* is thought to be negligible or rare because *E. coli* has not or has only a few serine/threonine or tyrosine kinases (24). CERT S315E exhibited 2–3-fold higher activity than that of the wild-type CERT control, whereas CERT ΔFFAT or the CERT S315E/ΔFFAT mutant exhibited less activity (Fig. 3*A*). These results indicated that the S315E mutation enhanced the function of CERT for the ER-to-Golgi transport of ceramide and that this enhanced function was dependent on the existence of the FFAT motif in CERT. To elucidate whether Ser-315 phosphorylation affected not only the affinity for VAP but also other functional domains of CERT, we analyzed inter-membrane transfer activity (attributed to the START domain) and PtdIns(4)P binding activity (attributed to the PH domain) in cell-free assay systems (Fig. 3, *B* and *C*). CERT S315E did not exhibit higher activity of ceramide transfer, whereas its PtdIns(4)P binding activity was marginally higher than that of the wild-type CERT control. However, these differences in activities between CERT S315E and the wild-type control were not distinct enough to account for the high activity of CERT S315E to support the ER-to-Golgi transport of ceramide in semi-intact cells. Collectively, we interpreted from these results that the high activity of CERT S315E for the ER-to-Golgi transport of ceramide was largely due to its stronger affinity for VAP and not any influence on the PH or START domains.

Influence of the Phosphorylation State of the SRM on the Phosphorylation of Ser-315—The phosphorylation of the SRM of CERT has been shown to repress both the functions of PH and START domains of CERT (14). Thus, we attempted to elucidate whether the phosphorylation state at the SRM influenced the phosphorylation of CERT at Ser-315. Various mutant constructs of HA-CERT were expressed in HeLa-S3 cells, and the phosphorylation states at Ser-315 were compared. All mutant constructs used here were expressed at a level similar to that of the wild-type control (Fig. 4*A, upper panel*). CERT S132A, which was defective in the phosphorylation of the SRM, was highly phosphorylated at Ser-315, although no significant differences were observed in the phosphorylation of Ser-315 between CERT 10E, which is an SRM-hyperphosphorylated mimicry by replacing all 10 serine/threonine residues in the SRM to glutamic acids, and the CERT wild-type control (Fig.

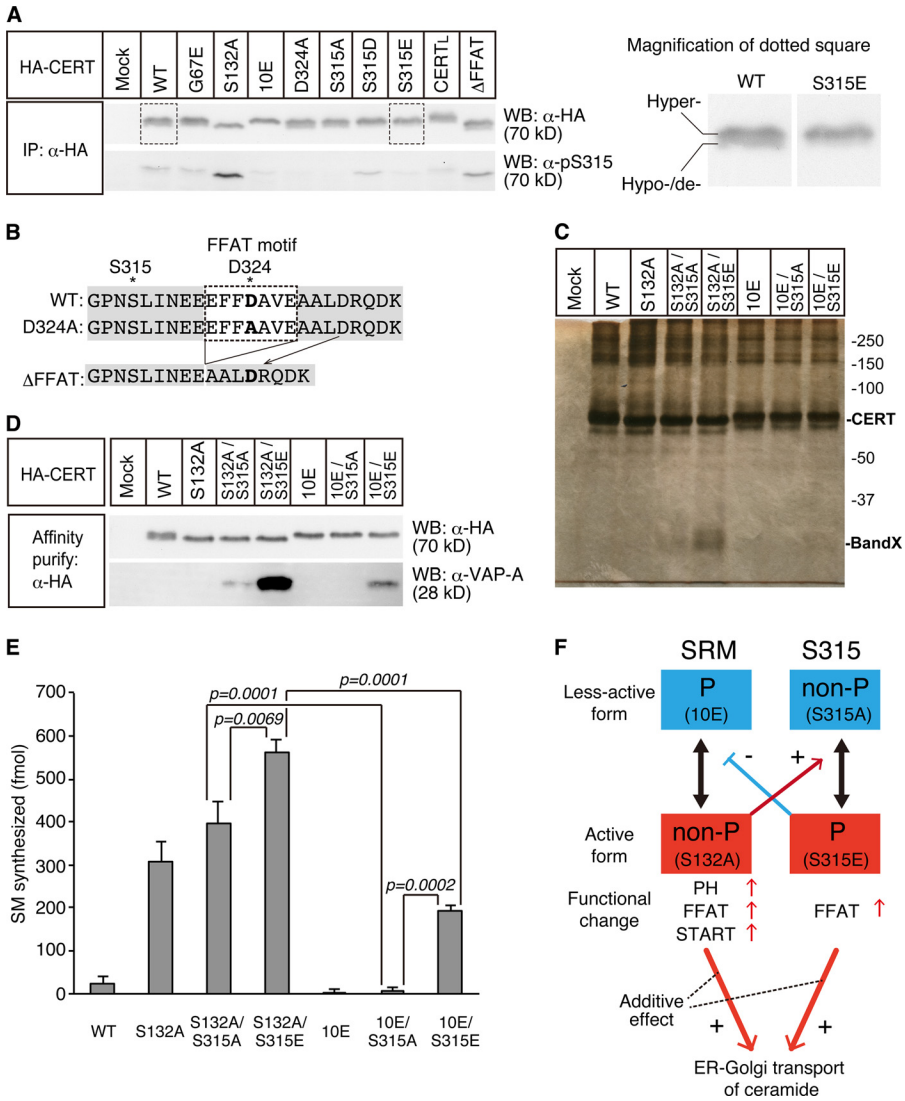

FIGURE 4. **Functional interactions between the SRM and Ser(P)-315 in CERT.** *A,* HeLa-S3 cells were transfected with an expression plasmid encoding HA-CERT WT, HA-CERT S315A, or an empty vector and cultured for 48 h before harvesting. Cell lysates were prepared by sonication with buffer A supplemented with 0.2% SDS and subjected to SDS-PAGE followed by Western blotting (*WB*) with the anti-HA antibody (α-*HA*) and anti-Ser(P)-315 antibody (α-*pS315*). The area enclosed with *dotted line* (CERT WT and CERT S315E) is enlarged in the *right panel* to show the doublet appearance of CERT more clearly. The *upper band* represents the hyper-phosphorylated form, and the *lower band* represents the hypo-phosphorylated or de-phosphorylated form of CERT at the SRM (14, 31). Experiments were performed at least three times, and similar results were obtained. Typical blot patterns are shown. *IP*, immunoprecipitated. *B,* amino acid sequences (312–335) around the FFAT motif of various human CERT constructs are shown. The core region of the FFAT motif is enclosed by a *dotted line*, and the *asterisk* represents the position of Ser-315, and the mutated residues are in *bold letters*. *C,* HA-tagged CERT WT and mutated CERT transiently expressed in HeLa-S3 cells were purified, subjected to SDS-PAGE, and analyzed by silver staining. CERT (70 kDa) and the putative endogenous VAP protein (marked by *Band X*) are indicated. The ladder bands in the high molecular range are most likely oligomers of CERT (41). *D,* purified proteins described in *C* were analyzed by Western blotting with the anti-HA antibody (α-*HA*) and anti-VAP-A antibody (α-*pS315*). *E,* purified CERT proteins (20 fmol) described in *C* were used to measure the ER-to-Golgi trafficking activity of ceramide in semi-intact LY-A cells as described previously (18). The data shown are the means ± S.D. from three experiments. The significance of changes was analyzed by the Student's *t* test, and *p* values are shown. *F,* hypothetical model of the functional regulation of CERT by the phosphorylation of the SRM and Ser-315 is depicted as follows: phosphorylated state (*P*), non-phosphorylated state (*non-P*), less-active form (*blue boxes*), and active form (*red boxes*). Typical mutations mimicking these states are shown in *parentheses*. The phosphorylation states of one region may mutually affect those of the other region. The de-phosphorylation of the SRM and the phosphorylation of Ser-315 additively enhance the activity of CERT to transport ceramide from the ER to the Golgi apparatus for the synthesis of SM.

4*A*, *lower panel*). In contrast, the G67E mutation in the PH domain, which is known to cause the loss of PtdIns(4)P binding activity (9), did not affect the phosphorylation state of Ser-315. It should also be noted that the phosphorylation at Ser-315 occurred in $CERT_L$, a large splicing isoform of CERT (or Goodpasture antigen-binding protein) (3, 25) as in CERT (Fig. 4*A*). These results suggested that the de-phosphorylation of the SRM could up-regulate the phosphorylation of Ser-315.

These results raised the possibility that the activation of CERT by the de-phosphorylation of the SRM compulsorily required the phosphorylation of Ser-315. To test this possibility, we expressed various mutant constructs of HA-CERT in HeLa-S3 cells, purified them by affinity chromatography, and analyzed their ability to transport ceramide from the ER to the Golgi apparatus within semi-intact cells. Silver staining of purified preparations in SDS-PAGE confirmed their purity (Fig. 4*C*). A band with an apparent molecular mass of ~28 kDa was clearly observed in the CERT S132A/S315E preparation (Fig. 4*C*). We expected this band to be VAP-A because the S315E mutation enhanced the interaction between CERT and VAP-A

and was also due to the apparent molecular mass of FLAG-VAP-A on Western blots being ~28 kDa (Fig. 1). This expectation was confirmed by Western blot analysis of the purified CERT preparations with anti-VAP-A antibodies (Fig. 4*D*). The highest level of co-purification of VAP-A with CERT was detected in the CERT S132A/S315E preparation, and a lower level of the co-purification was also detected in the CERT 10E/S315E preparation (Fig. 4*D*). These results suggested that the affinity of CERT for VAP was attenuated by the phosphorylation of the SRM (Fig. 4*F*). In addition, the efficient co-purification of VAP-A with CERT S132A/S315E (Fig. 4, *B* and *C*) suggested that a substantial population of the fully activated CERT was bound with VAP in cells, supporting our previous proposal that CERT functions mainly at the ER-to-Golgi membrane contact sites (13, 14, 26). We detected the marginal co-purification of VAP-A with CERT S132A/S315A, but did not for other CERT constructs (WT, S132A, 10E, and 10E/S315E) under the experimental conditions used (Fig. 4*D*). The reason why CERT S132A/S315A may have a higher affinity for VAP-A than CERT S132A remains unknown.

The ceramide transport activity of these HeLa cell-derived CERT preparations was assayed in semi-intact cells. The activities of both CERT S132A and CERT S132A/S315A were ~10-fold higher than that of the wild-type control, although no activity was detected for CERT 10E or CERT 10E/S315A (Fig. 4*E*), which is consistent with the findings of our previous study (14). Considering that the phosphorylation level of the SRM and Ser-315 of CERT expressed in HeLa cells could not be 100%, we focused on the double mutants (S132A/S315E, S132A/S315A, 10E/S315E, and 10E/S315A) for further quantitative analysis. CERT S132A/S315A exhibited higher activity than CERT 10E/S315A (Fig. 4*E*), which indicated that CERT could be activated by the de-phosphorylation of the SRM even without the phosphorylation of Ser-315. Likewise, CERT 10E/S315E showed higher activity than CERT 10E/S315A (Fig. 4*E*), which indicated that CERT could be activated by the phosphorylation of Ser-315 even without the de-phosphorylation of the SRM. CERT S132A/S315E showed the highest activity, the level of which was near the sum of the levels of CERT S132A/S315A and CERT 10E/S315E (Fig. 4*E*). Thus, the de-phosphorylation of the SRM and the phosphorylation of Ser-315 likely have the additive contribution to enhance the ceramide transport activity (Fig. 4*F*).

We could not formally eliminate the possibility that co-purified VAP-A promoted the activity of CERT constructs in semi-intact cells. However, even when CERT recombinants purified from *E. coli* (VAP-A or its ortholog is absent in *E. coli*) were used, the activity of CERT S315E was higher than that of wild-type CERT (Fig. 3*A*), which indicated that co-purified VAP-A was not essential for enhancing the ceramide transport activity of CERT S315E *in vitro*.

We obtained interesting results during our attempt to determine whether the phosphorylation of Ser-315 required the FFAT motif. Asp-324 is known to correspond to one of the conserved amino acid residues in the consensus FFAT motif (27), and VAP-A binding of CERT D324A was shown to be compromised (13). No discernible phosphorylation was observed at Ser-315 in CERT D324A (Fig. 4*A*). However, the phosphorylation of Ser-315 was observed in CERT ΔFFAT (which entirely lacked the core region of the FFAT motif) to a similar level to that in wild-type control (Fig. 4*A*). A possible explanation for these paradoxical results is that aspartic acid at position 324 rather than the FFAT motif itself may be crucial for the phosphorylation of Ser-315 because the amino acid residue of CERT ΔFFAT at the position 324 is aspartic acid (Figs. 1*C* and 4*B*). Further studies are needed to elucidate this possibility.

CERT S315E Mutant Induced the Formation of Intracellular Punctate Structures, to Which VAP-A Was Recruited—HA-CERT WT or HA-CERT with a point mutation on Ser-315 was stably expressed in HeLa-S3 cells, and their intracellular distribution was analyzed by indirect immunofluorescence staining with antibodies against HA and the Golgi marker GS28. All CERT constructs were distributed throughout the cytosol with preferential localization to the Golgi apparatus, and HA-CERT S315D and HA-CERT S315E were also localized on punctate structures, which were not observed when wild-type HA-CERT or HA-CERT S315A was expressed in HeLa-S3 cells (Fig. 5*A*). The localization of HA-CERT S315D and HA-CERT S315E to the punctate structures was not attributable to their excessive expression levels because Western blotting showed that the expression level of HA-CERT S315A (which could not induce the puncta) was slightly higher than those of HA-CERT S315D and/or HA-CERT S315E (data not shown). To further characterize these punctate structures, we examined the co-localization of HA-CERT S315E with endogenous VAP-A in HeLa-S3 cells. Endogenous VAP-A was distributed throughout the ER membranes, whereas a small amount of it was co-localized with punctate structures containing HA-CERT S315E (Fig. 5*B*). Under the same conditions, another ER marker protein-disulfide isomerase, membrane-associated ER marker Sec61β, Golgi marker GM130, or trans-Golgi network marker syntaxin-6 did not co-localize with the punctate structures (Fig. 5*C*), which indicated that the majority of the ER and Golgi apparatuses were not integrated into the CERT/VAP-A double-positive punctate structures. In addition, the punctate structures were not co-localized to LAMP-1 (a marker of late endosomes/lysosomes) or EEA1 (a marker of early endosomes) (Fig. 5*C*).

When HA-CERT S315E was highly expressed in HeLa-S3 cells by transient transfection (Fig. 6*A*), the appearance of punctate structures was clearer than the pattern observed in HA-CERT S315E-low expressing cells (Fig. 5, *A* and *B*). A large part of endogenous VAP-A was recruited to the punctate structures, to which HA-CERT S315E was localized (Fig. 6*A*). The overexpression of the HA-CERT S315E/ΔFFAT mutant (which was defective in VAP binding due to the deletion of the FFAT motif) did not induce punctate structures and was localized to the perinuclear Golgi apparatus (Fig. 6*A*). In addition, punctate structures induced by the expression of HA-CERT S315E were diminished when cells were treated with a small interfering RNA (siRNA) to VAP-A but not by control siRNA (Fig. 6*B*). Further reductions were observed when cells were treated with both VAP-A siRNA and VAP-B siRNA (Fig. 6*B*). When HA-CERT S315E/G67E (which lost PtdIns(4)P-binding activity due to a G67E mutation in the PH domain (9)) was expressed in

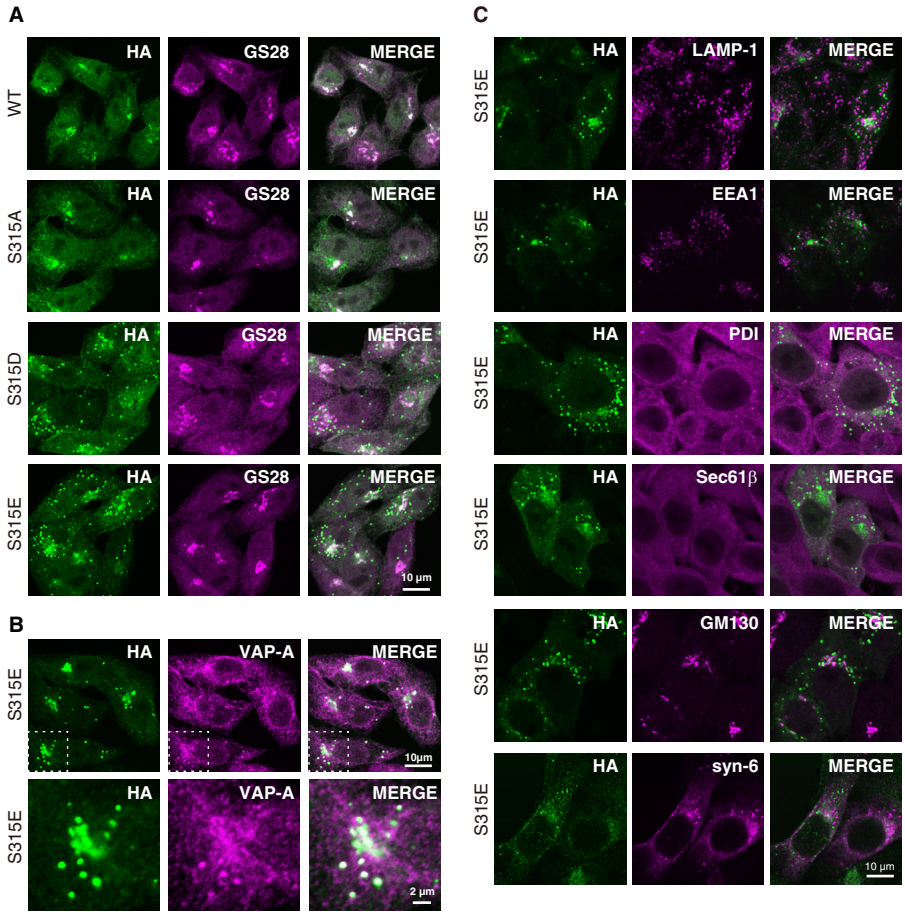

FIGURE 5. **Effects of Ser-315 phosphorylation on the intracellular distribution of CERT.** *A,* HeLa-S3 cells stably expressing HA-CERT WT or HA-CERT mutations were double-labeled with the anti-HA antibody (*green*) and anti-GS28 antibody (*magenta*) by indirect immunostaining and were then observed by confocal microscopy. Experiments were performed at least three times, and similar results were obtained. Typical staining patterns are shown. *B,* HeLa-S3 cells stably expressing HA-CERT S315E were double-labeled with the anti-HA antibody (*green*) and anti-VAP-A antibody (*magenta*) by indirect immunostaining and observed by confocal microscopy (*upper panel*). A high magnification of the selected region (*boxes with dotted line* in *upper panel*) is also shown (*lower panel*). *C,* HeLa-S3 cells stably expressing HA-CERT S315E were double-labeled with the anti-HA antibody (*green*) and the indicated antibodies (*magenta*) by indirect immunostaining and observed by confocal microscopy. The antibodies used were as follows: a late endosomal/lysosomal marker, *LAMP-1*; an early endosomal marker, *EEA1*; an ER marker, protein-disulfide isomerase, *PDI*; a membrane-associated ER marker, *Sec61β*; a Golgi marker, *GM130*; a *trans*-Golgi network marker, syntaxin-6 (*syn-6*). The *bar* indicates 10 μm.

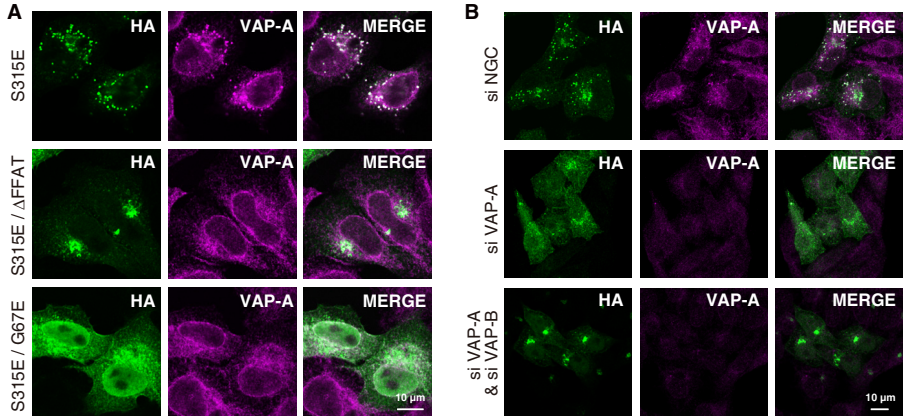

FIGURE 6. **Dependence of the punctate formation of CERT S315E on its PtdIns(4)P binding and VAP binding activities.** *A,* HeLa-S3 cells were transiently transfected with HA-CERT S315E, HA-CERT S315E/G67E, and HA-CERT S315E/ΔFFAT constructs and were then cultured for 24 h. Cells were double-labeled with the anti-HA antibody (*green*) and anti-VAP-A antibody (*magenta*) by indirect immunostaining and observed by confocal microscopy. The *bars* indicate 10 μm. *B,* HeLa-S3 cells stably expressing HA-CERT S315E were transfected with siRNA against VAP-A and incubated for 24 h. The cells were double-labeled with the anti-HA antibody (*green*) and anti-VAP-A antibody (*magenta*) by indirect immunostaining and observed by confocal laser-scanning microscope (Axio Observer Z1; Carl Zeiss) equipped with an LSM 700 ZEN system (Carl Zeiss) using a Plan-Apochromat 63×/1.4 Oil differential interference contrast objective lens. The *bar* indicates 10 μm.

HeLa-S3 cells, it exhibited endoplasmic reticular distribution like VAP-A and did not induce punctate structures (Fig. 6*A*).

DISCUSSION

This study showed that the FFAT motif-dependent interaction of CERT with VAP-A was enhanced by the phosphorylation of CERT at Ser-315. Analysis with various CERT mutant constructs revealed a positive correlation between its affinity for VAP-A and ceramide transport activity *in vitro* (Figs. 1–4). In addition, the phosphorylation at Ser-315 of CERT was promoted when cells were treated with ISP-1, a potent inhibitor of sphingolipid biosynthesis, or sphingomyelinase (Fig. 2). Collectively, these results strongly suggest that the ER-to-Golgi trafficking of ceramide is up-regulated by the phosphorylation of CERT at Ser-315 due to an enhancement in affinity for VAP, and this may occur in response to the perturbation of cellular sphingomyelin and/or other sphingolipids.

Mikitova and Levine (21) showed that many proteins have FFAT-like motifs, which are similar, but with one or two suboptimal substitutions, to the canonical FFAT motifs (EFFDA*X*E). They further suggested that, although an FFAT-like motif (TFFSAN) could not interact with VAP, the replacement of neutral amino acids to acidic amino acids in the motif (*e.g.* TFFSAN to EFFDAN) enabled the motif to weakly interact with VAP (21), which raised the possibility that the phosphorylation of FFAT-like motifs might affect the interaction of motif-containing proteins with VAP. FFAT-like motifs of STARD3/MNL64 and STARD3NL/MENTAL were recently found to be essential for association of these proteins with VAP to tether late endosomes and the ER (28). However, it remains unclear whether phosphorylation in or around FFAT-like motifs really occurs in cells. This study provides compelling evidence that *bona fide* phosphorylation at a specific serine (Ser-315) in the flanking region of the motif enhances the interaction of CERT with VAP-A in an FFAT motif-dependent manner (Figs. 1 and 2) and that the phosphorylation of CERT is relevant to the regulation of ceramide transport in semi-intact cells (Figs. 3*A* and 4*E*). Serine/threonine residues are frequently observed in the flanking region of FFAT motifs (21). Similar scenarios on the adjacent phosphorylation may occur in various FFAT motif-containing proteins to regulate their interaction with VAP.

We previously indicated that CERT was phosphorylated at multiple serine/threonine residues in the SRM (for the position of the SRM, see Fig. 1*A*) to down-regulate the ceramide trafficking function of CERT by repressing activities of the PH and START domains (Fig. 4*F*) (14). In this study, we demonstrated that CERT S132A/S315E exhibits more efficient VAP-A-binding than CERT 10E/S315E (Fig. 4, *C* and *D*), which suggests that the affinity of CERT for VAP is attenuated by the phosphorylation of the SRM (Fig. 4*F*). The result is consistent with our previous study showing that protein phosphatase 2Cε de-phosphorylates the SRM of CERT, which results in an increment of the interaction of CERT with VAP (29). In contrast, the phosphorylation of Ser-315 up-regulated the function of CERT by primarily enhancing the FFAT motif-dependent interaction between CERT and VAP (Figs. 1–4). The treatment of cells with ISP-1 or sphingomyelinase induced the de-phosphorylation of the SRM (14) and also the phosphorylation of Ser-315 (this study), which rendered CERT in a more active state. These results suggested that CERT was post-translationally regulated by at least two different kinase systems as follows: a system involving protein kinase D and casein kinase I, which is relevant to the phosphorylation of the SRM (30, 31), and a system relevant to the phosphorylation of Ser-315, whose responsible kinase(s) has yet to be identified.

We further demonstrated that the Ser-315-phosphorylated form was produced more in CERT S132A than in CERT 10E (Fig. 4*A*), which suggests that the de-phosphorylation of SRM promotes the phosphorylation of Ser-315 or attenuates the dephosphorylation of Ser(P)-315. Thus, the SRM and Ser-315 (along with the FFAT motif) appear to cross-talk for the functional regulation of CERT (Fig. 4*F*), even though these two regions are likely phosphorylated by different kinases.

When the CERT S315E mutant was expressed in HeLa-S3 cells, unknown punctate structures appeared, to which CERT and VAP-A were co-localized (Fig. 5, *A* and *B*). Such structures were not produced when CERT mutants defective in PtdIns(4) binding or VAP-A-binding were expressed or the expression of endogenous VAPs was suppressed (Fig. 6, *A* and *B*). These results suggest that these puncta may be CERT-connected complexes of VAP-embedded membranes and PtdIns(4)P-embedded membranes. Paradoxically, neither of the typical ER markers (protein-disulfide isomerase and Sec61β) or Golgi/*trans*-Golgi network markers (GS28, GM130, and syntaxin-6) co-localized with the punctate structures (Fig. 5). The structures could be condensed ER membranes enriched in VAP-A that might be induced by overexpression of active CERT. Alternatively, they could be relevant to the ER-Golgi membrane contact sites that might be composed of unrecognized microdomains devoid of typical ER and Golgi marker proteins. More studies, including electron microscopic analysis, are needed to elucidate this issue.

A novel model for the ER-to-Golgi transfer of oxysterol by oxysterol-binding protein (OSBP) has very recently been proposed (32). In this model, OSBP was shown to transfer oxysterol from the ER to the Golgi apparatus and, in turn, transfer PtdIns(4)P from the Golgi and ER at membrane contact sites by a tight coupling mechanism. The overall module architecture of CERT is similar to that of OSBP with an N-terminal PtdIns(4)P-specific PH domain, C-terminal lipid-transfer domain, and FFAT motif between them, although no similarities have been observed in the primary structures of the lipid-transfer domains. OSBP was shown to have the potential to connect the ER with the Golgi apparatus (32). Thus, various proteins having both a PtdIns(4)P-specific PH domain and FFAT motif may contribute to the formation of ER-Golgi membrane contact sites in cells, and the yet unidentified phosphorylation/dephosphorylation system responsible for the phosphorylation of CERT Ser-315 might play a role in regulatory formation of ER-Golgi membrane contact sites.

Recent studies showed that CERT is involved in various biological events. For example, the inhibition of CERT was shown to re-sensitize various types of drug-resistant cancer cells to anti-tumor drugs (33). The expression of a constitutively SRM-dephosphorylated form of CERT (CERT S132A) resulted in the enhanced secretion of monoclonal antibodies in CHO cells

(34). In addition, a dysfunction in CERT may be relevant to the palmitate-induced inhibition of insulin gene expression in islet β-cells (35). CERT also seems to participate in the synthesis of ceramide 1-phosphate in the Golgi apparatus (36), and ceramide 1-phophate produced in the Golgi site is likely to be transported to the plasma membrane by its transfer protein for the regulation of bioactivity of ceramide 1-phosphate (37). Moreover, CERT was shown to be required for several types of intracellular parasites such as the obligate intracellular bacterial parasite *Chlamydia* species (38, 39) and hepatitis C-type virus (40) to propagate in human host cells. Our findings on the up-regulation and down-regulation of CERT may be contributed to wider fields of biological sciences.

Acknowledgment—We thank Neale Ridgway (Department of Biochemistry and Molecular Biology, Dalhousie University, Canada) for helpful discussion. We also thank Nario Tomishige of our laboratory (present affiliation: RIKEN, Japan) for his contribution to the construction of CERT Ser-315 mutants.

REFERENCES

1. Pewzner-Jung, Y., Ben-Dor, S., and Futerman, A. H. (2006) When do Lasses (longevity assurance genes) become CerS (ceramide synthases)? Insights into the regulation of ceramide synthesis. *J. Biol. Chem.* **281,** 25001–25005
2. Mullen, T. D., Hannun, Y. A., and Obeid, L. M. (2012) Ceramide synthases at the centre of sphingolipid metabolism and biology. *Biochem. J.* **441,** 789–802
3. Hanada, K. (2013) Co-evolution of sphingomyelin and the ceramide transport protein CERT. *Biochim. Biophys. Acta*, in press, 10.1016/j.bbalip/2013.06.006
4. van Meer, G., Voelker, D. R., and Feigenson, G. W. (2008) Membrane lipids: Where they are and how they behave. *Nat. Rev. Mol. Cell Biol.* **9,** 112–124
5. Holthuis, J. C., and Levine, T. P. (2005) Lipid traffic: Floppy drives and a superhighway. *Nat. Rev. Mol. Cell Biol.* **6,** 209–220
6. Ishibashi, Y., Kohyama-Koganeya, A., and Hirabayashi, Y. (2013) New insights on glucosylated lipids: Metabolism and functions. *Biochim. Biophys. Acta* **1831,** 1475–1485
7. Kolter, T., and Sandhoff, K. (2006) Sphingolipid metabolism diseases. *Biochim. Biophys. Acta* **1758,** 2057–2079
8. Merrill, A. H., Jr. (2011) Sphingolipid and glycosphingolipid metabolic pathways in the era of sphingolipidomics. *Chem. Rev.* **111,** 6387–6422
9. Hanada, K., Kumagai, K., Yasuda, S., Miura, Y., Kawano, M., Fukasawa, M., and Nishijima, M. (2003) Molecular machinery for non-vesicular trafficking of ceramide. *Nature* **426,** 803–809
10. Sugiki, T., Takeuchi, K., Yamaji, T., Takano, T., Tokunaga, Y., Kumagai, K., Hanada, K., Takahashi, H., and Shimada, I. (2012) Structural basis for the Golgi association by the pleckstrin homology domain of the ceramide trafficking protein (CERT). *J. Biol. Chem.* **287,** 33706–33718
11. Kumagai, K., Yasuda, S., Okemoto, K., Nishijima, M., Kobayashi, S., and Hanada, K. (2005) CERT mediates intermembrane transfer of various molecular species of ceramides. *J. Biol. Chem.* **280,** 6488–6495
12. Kudo, N., Kumagai, K., Tomishige, N., Yamaji, T., Wakatsuki, S., Nishijima, M., Hanada, K., and Kato, R. (2008) Structural basis for specific lipid recognition by CERT responsible for nonvesicular trafficking of ceramide. *Proc. Natl. Acad. Sci. U.S.A.* **105,** 488–493
13. Kawano, M., Kumagai, K., Nishijima, M., and Hanada, K. (2006) Efficient trafficking of ceramide from the endoplasmic reticulum to the Golgi apparatus requires a VAMP-associated protein-interacting FFAT motif of CERT. *J. Biol. Chem.* **281,** 30279–30288
14. Kumagai, K., Kawano, M., Shinkai-Ouchi, F., Nishijima, M., and Hanada, K. (2007) Interorganelle trafficking of ceramide is regulated by phosphorylation-dependent cooperativity between the PH and START domains of CERT. *J. Biol. Chem.* **282,** 17758–17766
15. Hanada, K., Kumagai, K., Tomishige, N., and Yamaji, T. (2009) CERT-mediated trafficking of ceramide. *Biochim. Biophys. Acta* **1791,** 684–691
16. Miyake, Y., Kozutsumi, Y., Nakamura, S., Fujita, T., and Kawasaki, T. (1995) Serine palmitoyltransferase is the primary target of a sphingosine-like immunosuppressant, ISP-1/myriocin. *Biochem. Biophys. Res. Commun.* **211,** 396–403
17. Kumagai, K., Nishijima, M., and Hanada, K. (2012) Reconstitution assay system for ceramide transport with semi-intact cells. *Methods Cell Biol.* **108,** 117–129
18. Funakoshi, T., Yasuda, S., Fukasawa, M., Nishijima, M., and Hanada, K. (2000) Reconstitution of ATP- and cytosol-dependent transport of *de novo* synthesized ceramide to the site of sphingomyelin synthesis in semi-intact cells. *J. Biol. Chem.* **275,** 29938–29945
19. Dowler, S., Currie, R. A., Campbell, D. G., Deak, M., Kular, G., Downes, C. P., and Alessi, D. R. (2000) Identification of pleckstrin-homology-domain-containing proteins with novel phosphoinositide-binding specificities. *Biochem. J.* **351,** 19–31
20. Furuita, K., Jee, J., Fukada, H., Mishima, M., and Kojima, C. (2010) Electrostatic interaction between oxysterol-binding protein and VAMP-associated protein A revealed by NMR and mutagenesis studies. *J. Biol. Chem.* **285,** 12961–12970
21. Mikitova, V., and Levine, T. P. (2012) Analysis of the key elements of FFAT-like motifs identifies new proteins that potentially bind VAP on the ER, including two AKAPs and FAPP2. *PLoS One* **7,** e30455
22. Olsen, J. V., Blagoev, B., Gnad, F., Macek, B., Kumar, C., Mortensen, P., and Mann, M. (2006) Global, *in vivo*, and site-specific phosphorylation dynamics in signaling networks. *Cell* **127,** 635–648
23. Hanada, K., Yamato, I., and Anraku, Y. (1985) Identification of proline carrier in *Escherichia coli* K-12. *FEBS Lett.* **191,** 278–282
24. Shi, L., Potts, M., and Kennelly, P. J. (1998) The serine, threonine, and/or tyrosine-specific protein kinases and protein phosphatases of prokaryotic organisms: A family portrait. *FEMS Microbiol. Rev.* **22,** 229–253
25. Raya, A., Revert-Ros, F., Martinez-Martinez, P., Navarro, S., Rosello, E., Vieites, B., Granero, F., Forteza, J., and Saus, J. (2000) Goodpasture antigen-binding protein, the kinase that phosphorylates the goodpasture antigen, is an alternatively spliced variant implicated in autoimmune pathogenesis. *J. Biol. Chem.* **275,** 40392–40399
26. Hanada, K. (2006) Discovery of the molecular machinery CERT for endoplasmic reticulum-to-Golgi trafficking of ceramide. *Mol. Cell. Biochem.* **286,** 23–31
27. Loewen, C. J., Roy, A., and Levine, T. P. (2003) A conserved ER targeting motif in three families of lipid binding proteins and in Opi1p binds VAP. *EMBO J.* **22,** 2025–2035
28. Alpy, F., Rousseau, A., Schwab, Y., Legueux, F., Stoll, I., Wendling, C., Spiegelhalter, C., Kessler, P., Mathelin, C., Rio, M. C., Levine, T. P., and Tomasetto, C. (2013) STARD3 or STARD3NL and VAP form a novel molecular tether between late endosomes and the ER. *J. Cell Sci.* **126,** 5500–5512
29. Saito, S., Matsui, H., Kawano, M., Kumagai, K., Tomishige, N., Hanada, K., Echigo, S., Tamura, S., and Kobayashi, T. (2008) Protein phosphatase 2Cε is an endoplasmic reticulum integral membrane protein that dephosphorylates the ceramide transport protein CERT to enhance its association with organelle membranes. *J. Biol. Chem.* **283,** 6584–6593
30. Fugmann, T., Hausser, A., Schöffler, P., Schmid, S., Pfizenmaier, K., and Olayioye, M. A. (2007) Regulation of secretory transport by protein kinase D-mediated phosphorylation of the ceramide transfer protein. *J. Cell Biol.* **178,** 15–22
31. Tomishige, N., Kumagai, K., Kusuda, J., Nishijima, M., and Hanada, K. (2009) Casein kinase Iγ2 down-regulates trafficking of ceramide in the synthesis of sphingomyelin. *Mol. Biol. Cell* **20,** 348–357
32. Mesmin, B., Bigay, J., Moser von Filseck, J., Lacas-Gervais, S., Drin, G., and Antonny, B. (2013) A four-step cycle driven by PI(4)P hydrolysis directs sterol/PI(4)P exchange by the ER-Golgi tether OSBP. *Cell* **155,** 830–843
33. Swanton, C., Marani, M., Pardo, O., Warne, P. H., Kelly, G., Sahai, E., Elustondo, F., Chang, J., Temple, J., Ahmed, A. A., Brenton, J. D., Downward, J., and Nicke, B. (2007) Regulators of mitotic arrest and ceramide metabolism are determinants of sensitivity to paclitaxel and other chemo-

therapeutic drugs. *Cancer Cell* **11,** 498–512
34. Florin, L., Pegel, A., Becker, E., Hausser, A., Olayioye, M. A., and Kaufmann, H. (2009) Heterologous expression of the lipid transfer protein CERT increases therapeutic protein productivity of mammalian cells. *J. Biotechnol.* **141,** 84–90
35. Guo, J., Zhu, J. X., Deng, X. H., Hu, X. H., Zhao, J., Sun, Y. J., and Han, X. (2010) Palmitate-induced inhibition of insulin gene expression in rat islet beta-cells involves the ceramide transport protein. *Cell. Physiol. Biochem.* **26,** 717–728
36. Lamour, N. F., Stahelin, R. V., Wijesinghe, D. S., Maceyka, M., Wang, E., Allegood, J. C., Merrill, A. H., Jr., Cho, W., and Chalfant, C. E. (2007) Ceramide kinase uses ceramide provided by ceramide transport protein: Localization to organelles of eicosanoid synthesis. *J. Lipid Res.* **48,** 1293–1304
37. Simanshu, D. K., Kamlekar, R. K., Wijesinghe, D. S., Zou, X., Zhai, X., Mishra, S. K., Molotkovsky, J. G., Malinina, L., Hinchcliffe, E. H., Chalfant, C. E., Brown, R. E., and Patel, D. J. (2013) Non-vesicular trafficking by a ceramide-1-phosphate transfer protein regulates eicosanoids. *Nature* **500,** 463–467
38. Derré, I., Swiss, R., and Agaisse, H. (2011) The lipid transfer protein CERT interacts with the *Chlamydia* inclusion protein IncD and participates to ER-*Chlamydia* inclusion membrane contact sites. *PLoS Pathog.* **7,** e1002092
39. Elwell, C. A., Jiang, S., Kim, J. H., Lee, A., Wittmann, T., Hanada, K., Melancon, P., and Engel, J. N. (2011) *Chlamydia trachomatis* co-opts GBF1 and CERT to acquire host sphingomyelin for distinct roles during intracellular development. *PLoS Pathog.* **7,** e1002198
40. Amako, Y., Syed, G. H., and Siddiqui, A. (2011) Protein kinase D negatively regulates hepatitis C virus secretion through phosphorylation of oxysterol-binding protein and ceramide transfer protein. *J. Biol. Chem.* **286,** 11265–11274
41. Charruyer, A., Bell, S. M., Kawano, M., Douangpanya, S., Yen, T. Y., Macher, B. A., Kumagai, K., Hanada, K., Holleran, W. M., and Uchida, Y. (2008) Decreased ceramide transport protein (CERT) function alters sphingomyelin production following UVB irradiation. *J. Biol. Chem.* **283,** 16682–16692